

The Combined Method of Dynamic Analysis of the «Soil-Structure» Systems at Aircraft Crash onto Civil Structure of NPP.

K. Ilin, V. Korotkov

JSC Atomenergoproekt, Moscow

Purpose of this paper is to determine response spectra in locations of components in the reactor building of nuclear plant VVER-1000 in case of aircraft crash (AC). Crash of aircraft PHANTOM is considered here. However methodology taken in this paper can be extended to beyond-the-design basis accident that is crash of large commercial aircraft of BOEING-747 type.

Code ABAQUS was applied for solution of the above-mentioned problem. Since aircraft crash causes nonlinear strain in shock area of concrete, we used the specially developed model of concrete in ABAQUS that is BRITTLE CRACKING MODEL, which enabled us to consider cracking of concrete and plastic strain of rebars.

Spatial model of the building was developed for the analysis; the model duplicates the complex inner structure of the building that enables simulation in true geometry.

Soil was analysed on the basis of three-dimension elements of continuous medium that allows simulating soil lamination. Previously the analyses of AC response spectra considered homogeneous soil.

It would be impossible to solve the problem with an ordinary personal computer because of demand on enormous main storage. Therefore efficient cluster of JSC ATOMENERGOPROEKT was utilized.

1. Methodology for Calculations of Soil-Structure

At present in analyses of soil-structure system at aircraft shock the soil basis is modelled as springs and dampers located under the building foundation. Characteristics of such spring-damper supports are determined for homogeneous elastic half-space by the formulas given in ASCE standards [1]. However is soil feature considerably heterogeneous nature, previously applied formulas from ASCE are unsuitable.

For the dynamic study of the reactor building with regard to complicated soil basis and similarly complicated its inner structure we could develop united finite-element model of the soil-structure system and solve problem in one step (implementation of direct solution). Spatial finite -element model of the system consisting of shell/plate elements for external structure and three-dimension elements of continuous medium for simulation of soil basis contains more than a million degrees of freedom and large width of band of stiffness matrix. Therefore solution of such problem with nonlinear behaviour of concrete will take long time.

That is why the idea is to solve the problem in two steps. At the first step we assume that the building is perfectly rigid and feature only inertia, and soil will be simulated by elements of continuous medium, which refer to the complicated structure of soil. At the second step we shall simulate the building on the basis of shell/plate elements, and we shall represent influence of soil as equivalent stiffness (6 springs) and equivalent damping (6 dampers), characteristics of which are determined in the first step.

In order to obtain equivalent linear stiffness as the initial factor, a unit deflection was applied, acting to stamp (see Figure 1), in geometric centre in the directions of linear degrees of freedom. Single turning angles were applied to obtain equivalent angular stiffness.

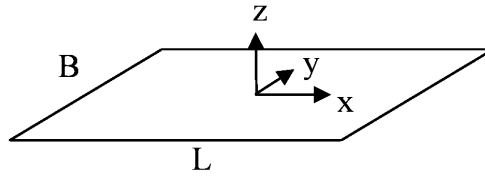


Figure 1. Stamp.

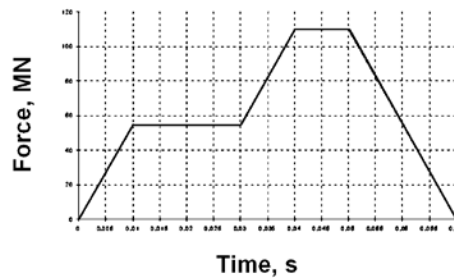


Figure 2 Impulse of dynamic impact from aircraft Phantom RF 4E.

In the analysis of equivalent damping in soil, the impulse impact from Phantom was applied to the stamp (see Figure 2) and after consideration of oscillating process the logarithmic decrement of damping was determined, which characterise radiation damping. Noteworthy, that just radiation damping will be determined in such study, since initial data for other types of damping were not used.

Sizes of stamp simulating the perfectly rigid foundation slab are as follows: $L = 76 \text{ m}$, $B = 54 \text{ m}$. Building mass is $m = 254432 \text{ t}$, and inertia moments around axes passing through geometric centre of the foundation slab are: $I_{xx} = 350217000 \text{ t}\cdot\text{m}^2$, $I_{yy} = 337464000 \text{ t}\cdot\text{m}^2$, $I_{zz} = 163827000 \text{ t}\cdot\text{m}^2$.

At the side boundaries of soil parallelepiped, which simulates soil basis, some special infinite elements were installed in order to absorb transient waves, and lower boundaries were restrained rigidly. Taking into account the above-mentioned and also from considerations that wave caused in soil from stamp oscillation must not be distorted because of reflection from boundary of soil parallelepiped at least during two oscillation periods, we took the following size of the soil parallelepiped: $L = B = 600 \text{ m}$, $H = 300 \text{ m}$. Ballast cushion properties were taken as soil characteristics: $V_s = 500 \text{ m/s}$, $\rho = 2 \text{ t/m}^3$ and $\nu = 0.4$ and homogeneous soil was taken for development of the methodology.

It shall be pointed out, that requirement to have non-distortion of wave is necessary for application of logarithmic decrement method in the course of determination of equivalent damping. Taking into account the above-mentioned, a mathematic model was developed for soil parallelepiped, consisting of eight-node cubic elements of 10 m size.

As a result of analysis with the use of ABAQUS the equivalent stiffness and equivalent damping presented in Table 1 were obtained for the stamp, vibrating on soil parallelepiped to

simulate homogeneous elastic half-space. Here the relevant stiffness and damping are presented, having been obtained by impedance functions from ASCE.

Table 1. Comparative analysis of equivalent stiffness and damping for homogeneous half-space.

	Equivalent stiffness			Equivalent damping	
	ASCE	ABAQUS		ASCE	ABAQUS
$k_x, t/m$	$8.2 \cdot 10^6$	$10.9 \cdot 10^6$	$b_x, t \cdot s/m$	$3.4 \cdot 10^5$ (38%)	$4.4 \cdot 10^5$ (42%)
$k_y, t/m$	$9.2 \cdot 10^6$	$11.3 \cdot 10^6$	$b_y, t \cdot s/m$	$3.8 \cdot 10^5$ (40%)	$4.9 \cdot 10^5$ (46%)
$k_z, t/m$	$1.2 \cdot 10^7$	$1.5 \cdot 10^7$	$b_z, t \cdot s/m$	$7.1 \cdot 10^5$ (66%)	$7.4 \cdot 10^5$ (60%)
$k_{\varphi_x}, t \cdot m$	$8.5 \cdot 10^9$	$10.4 \cdot 10^9$	$b_{\varphi_x}, t \cdot s \cdot m$	$9.0 \cdot 10^7$ (8%)	$8.4 \cdot 10^7$ (7%)
$k_{\varphi_y}, t \cdot m$	$1.4 \cdot 10^{10}$	$1.6 \cdot 10^{10}$	$b_{\varphi_y}, t \cdot s \cdot m$	$2.4 \cdot 10^8$ (17%)	$2.3 \cdot 10^8$ (15%)
$k_{\varphi_z}, t \cdot m$	$1.4 \cdot 10^{10}$	$1.7 \cdot 10^{10}$	$b_{\varphi_z}, t \cdot s \cdot m$	$1.5 \cdot 10^8$ (15%)	$2.3 \cdot 10^8$ (22%)

In the Table 1 damping percentage in brackets were determined as share of the critical damping value.

From the comparative analysis of equivalent stiffness it is evident that analysis done with the use of ABAQUS for all the cases give results greater than the equivalent stiffness obtained in ASCE formulas for the semi-infinite space. One among reasons of higher results is that semi-infinite space was confined by actual size of soil parallelepiped. However if we increase this size, then decrease of the equivalent stiffness will be negligible (around 7%). In particular, k_z will be $1.4 \cdot 10^7 t/m$. In such case it is require to develop mathematic model of soil for large size, but as a result we still have an insurmountable difference of around 15% between results with regard to the equivalent stiffnesses because of approximate nature of ASCE formulas.

Let us review in details method of coming to the equivalent damping given in Table 1. With this aim we studied free oscillations of the stamp after aircraft crash. Figure 4-9 demonstrate damping-time curves.

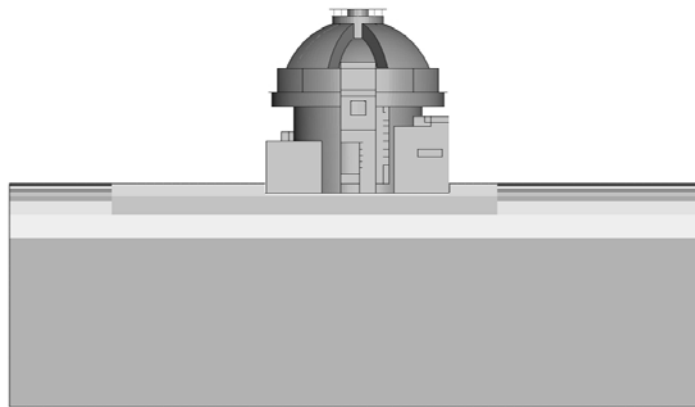


Figure 3. General view of soil-structure system.

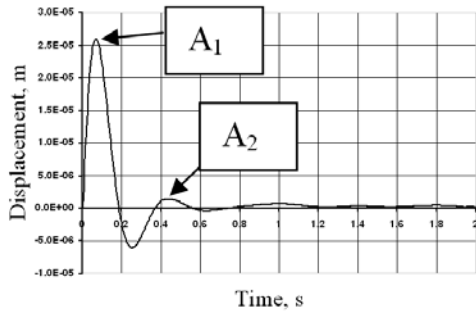


Figure 4. Damping at u_x .

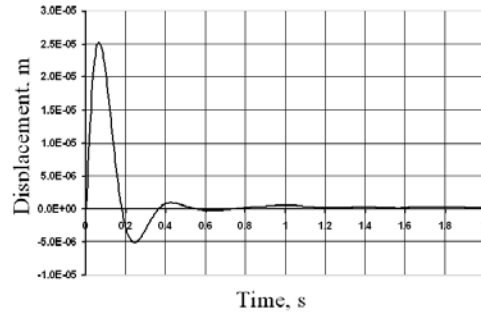


Figure 7. Damping at u_{φ_x} .

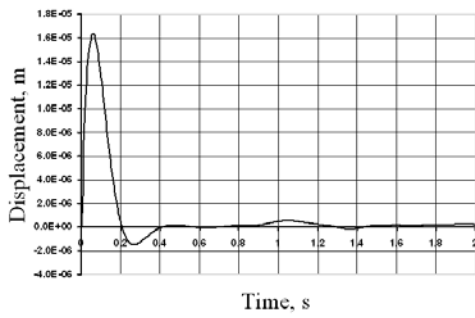


Figure 5. Damping at u_y .

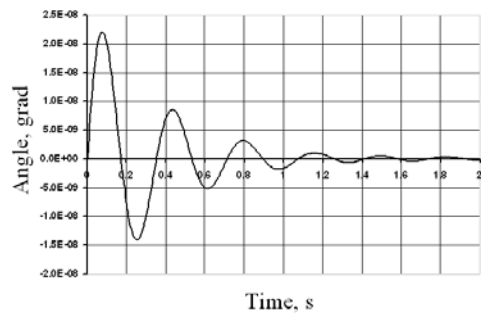


Figure 8. Damping at u_{φ_y} .

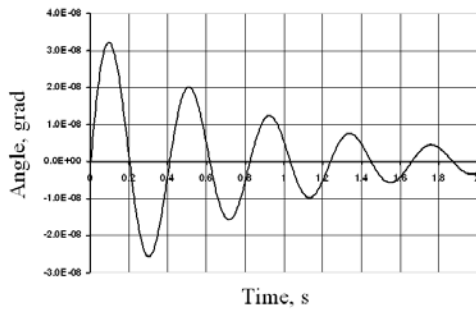


Figure 6. Damping at u_z .

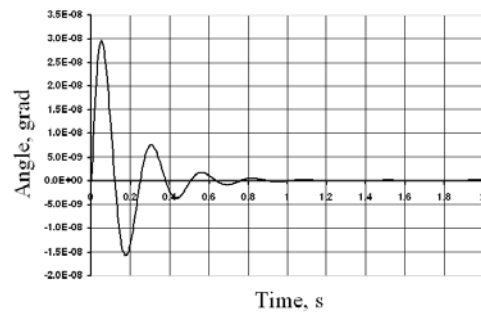


Figure 9. Damping at u_{φ_z} .

$\{U_x, U_y, U_z, U_{\varphi_x}, U_{\varphi_y}, U_{\varphi_z}\}$ - components of displacements

Using these curves we define damping logarithmic decrement as follows:

$$\eta = \ln \frac{A_1}{A_2} = \frac{2\pi\xi}{\sqrt{1-\xi^2}}, \quad (1)$$

where A_1 and A_2 - amplitudes of the first and second oscillations and ξ is relative damping. Here with we easily obtain:

$$\xi = \frac{\eta}{\sqrt{4\pi^2 + \eta^2}}. \quad (2)$$

Using Equation 2, the equivalent damping was obtained to be as follows:

$$b_i = 2\xi_i \sqrt{k_i m_i}, \quad (3)$$

where $i = x, y, z, \varphi_x, \varphi_y, \varphi_z$ and m_i and ξ_i represent building mass and moment of inertia, and relative damping in the process of translational and rotational displacements, accordingly.

Let us alternatively review obtaining of frequency-dependent characteristics of stiffness and damping for this problem. For this, as initial impact to stamp we apply displacement, varying according the harmonic law with single amplitude, and frequency, varying from 0.5 Hz to 30 Hz through 0.5 Hz steps. As a result we come to dynamic reaction. Phase difference (φ)

between amplitude of reaction force (RF) and amplitude of displacement we define graphically. As a result, values of dynamic stiffness (k) and damping (b) for the fixed value of external impact frequency (ω) was determined by the following formulas:

$$k = RF \cos \varphi \quad (4)$$

$$b = \frac{RF \sin \varphi}{\omega}. \quad (5)$$

Figure 10 and 11 demonstrate the dynamic stiffness and damping at vertical vibrations of the stamp dependent on frequency of driving force. As seen from Figure 10, stiffness at low oscillation frequencies (0.5 Hz) is $1.4 \cdot 10^7 \text{ t/m}$ that perfectly fits earlier analyses done by static method.

In compliance with Figure 11, damping is $8.3 \cdot 10^5 \text{ t}\cdot\text{s/m}$, which by 19% differs from the ASCE results. Swaying of oscillations at high frequencies is also seen in Figure 11. It happens due to FE rough mesh used in simulation of soil that ensures trustworthy solution at frequencies not greater than $5\text{-}10 \text{ Hz}$. However for this study such FE mesh is quite ample.

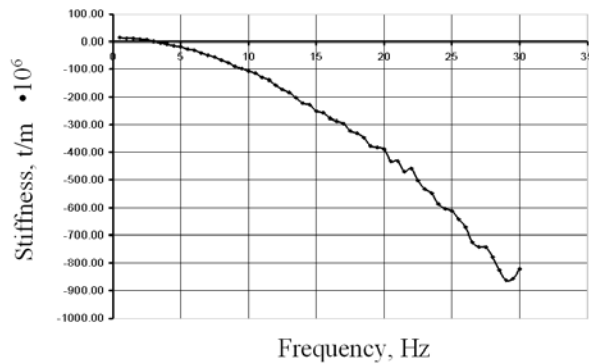


Figure 10. Dependence of the dynamic stiffness on frequency of harmonic impact.

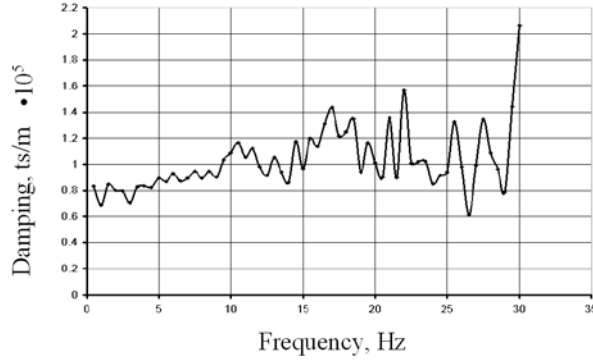


Figure 11. Dependence of dynamic damping on frequency of harmonic impact.

On the basis of the study we can come to conclusion that method of static stiffness and logarithmic damping decrement gives trustworthy results, if to compare with ASCE formulas, and frequency-dependent characteristics of stiffness and damping, and can be applied for calculations of stiffness and damping in laminated soil basis after aircraft crash. This method is more preferable than application of frequency-dependent characteristics, since the resultant equivalent stiffness and damping can easily be applied in timing methods of the dynamic analysis. When we use frequency-dependent characteristics, it is constantly a question about transition of characteristics from frequency into timing space.

With regard to reasons of difference between results of calculations done by static stiffness and logarithmic damping decrement method and calculations according to ASCE, as it was mentioned above; the difference happens because of approximate nature of methods used to determine the equivalent stiffness and damping according to ASCE.

Let us review the methodological aspects of direct integration method applied in the dynamic analysis. The main equation of movement of soil-structure system looks as follows:

$$KU_i + C\dot{U}_i + M\ddot{U}_i = P(t) \quad (6)$$

In Equation 6, U_i , \dot{U}_i and \ddot{U}_i are vectors of full displacements, velocities and accelerations of the system, and $P(t)$ is impact shown in Figure 2.

$K = K_1 + K_2$, where K_1 and K_2 are partial matrices of structure and soil stiffness.

$C = C_1 + C_2$, where C_1 is partial damping matrix related to viscous friction in the system and calculated according to Reyleigh's formula:

$$C_1 = \alpha M + \beta K, \quad (7)$$

and C_{21} is partial acoustic damping matrix, which characterise energy release from oscillating building into soil. Values K_2 and C_2 consist of components of the equivalent stiffness and damping presented in Table 1:

$K_2 = \{k_x, k_y, k_z, k_{\varphi_x}, k_{\varphi_y}, k_{\varphi_z}\}$ and $C_2 = \{b_x, b_y, b_z, b_{\varphi_x}, b_{\varphi_y}, b_{\varphi_z}\}$, M is the structure mass matrix.

Some details of this approach are set forth in [2].

2. Determination of the equivalent stiffness and damping for laminated soil base

Let us apply the above-described approach to determine the equivalent stiffness and damping for actual soil. General view of the soil-structure system is given in Figure 3.

Soil characteristics were determined based on the engineering-geological sections and tables with the calculated physical-mechanical and dynamic properties of soil. Based on these data the most significant layers were defined at depth up to 250 m. Based on the results of above studies the following sizes are obtained for soil parallelepiped under the building: $L = B = 600$ m and $H = 250$ m.

Soil layers used in calculations feature the characteristics given in Table 2.

Table 2. Soil properties under footing of the building.

EGE number	Soil description	Layer thickness, m	Density ρ , tonne/m^3	Velocity of shear waves V_s , m/s	Poisson's ratio, ν	Modulus of elasticity E , tonne/m^2
1b	Filled-up compacted sand-gravel soils	0.95	2.04	230	0.40	30000
5	Clays, lean days	0.90	2.02	390	0.45	89000
6	Clays, lean days	1.30	1.96	250	0.46	35000
8(8a)	Sandy loams, fine sands	1.40	2.02	450	0.45	10300
9a	Sandy loams, fine sands	1.70	2.00	520	0.44	14100
9	Dusty sands, fine sands, mean sands,	4.80	1.93	660	0.42	224000
12,13	Pebble with sand filler	8.30	2.29	700	0.43	267000
15	Marl	230.65	2.21	900	0.38	470000
1a	Ballast cushion above groundwater level	4.55	2.25	340	0.38	68000
1a	Ballast cushion below groundwater level	6.50	2.31	500	0.43	154000

The equivalent stiffness and damping were calculated for the stamp placed on the laminated soil base with the use of data given in this Table with help of ABAQUS according to the above-described methods. These data are given in Table 3.

Table 3. The equivalent stiffness and damping for laminated soil base.

	Equivalent stiffness		Equivalent damping
$k_x, \text{t/m}$	$1.6 \cdot 10^7$	$b_x, \text{ts/m}$	$2.5 \cdot 10^5$ (19%)
$k_y, \text{m/m}$	$1.7 \cdot 10^7$	$b_y, \text{ts/m}$	$3.0 \cdot 10^5$ (22%)
$k_z, \text{m/m}$	$4.2 \cdot 10^7$	$b_z, \text{ts/m}$	$9.4 \cdot 10^5$ (45%)
$k_{\varphi_x}, \text{t}\cdot\text{m}$	$1.4 \cdot 10^{10}$	$b_{\varphi_x}, \text{ts}\cdot\text{m}$	$2.6 \cdot 10^7$ (2%)
$k_{\varphi_y}, \text{t}\cdot\text{m}$	$2.8 \cdot 10^{10}$	$b_{\varphi_y}, \text{ts}\cdot\text{m}$	$11.1 \cdot 10^7$ (5.6%)
$k_{\varphi_z}, \text{t}\cdot\text{m}$	$1.7 \cdot 10^{10}$	$b_{\varphi_z}, \text{ts}\cdot\text{m}$	$7.9 \cdot 10^7$ (7%)

As is seen from Table 3, all the equivalent stiffness for laminated soil is greater than the equivalent stiffness for ballast cushion given in Table 1. The reason is that under ballast cushion there are layers with higher stiffness properties.

Comparing equivalent dampings it is evident that all the damping components, except for b_z calculated according to ABAQUS are lower than what is obtained according to ASCE. It shall be noted that the equivalent stiffness and damping indicated in Table 3 were obtained according to ABAQUS with the use of three-dimensional model of soil base with account of soil lamination. For determination of the equivalent damping we used curves of stamp oscillations on laminated soil, which are shown in Figure 12-17.

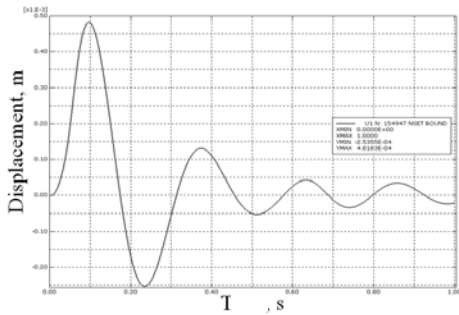


Figure 12. Damping at u_x .

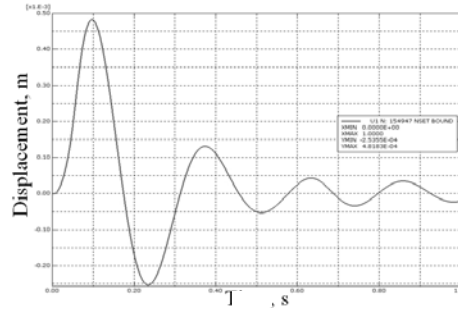


Figure 15. Damping at u_{ϕ_x} .

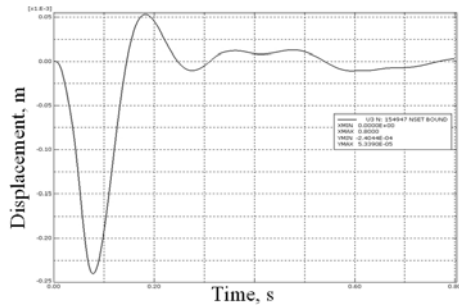


Figure 13. Damping at u_y .

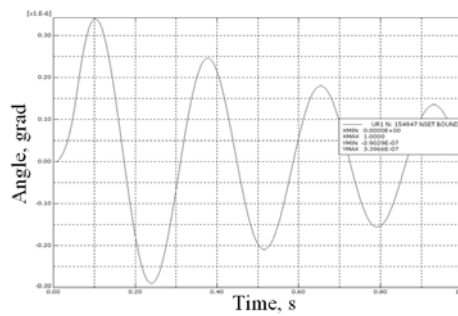


Figure 16. Damping at u_{ϕ_y} .

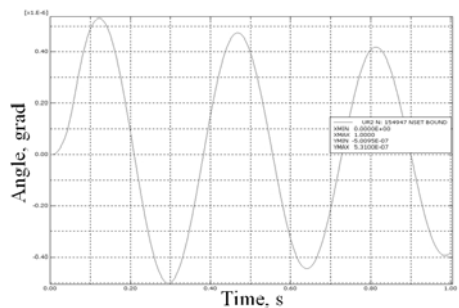


Figure 14. Damping at u_z .

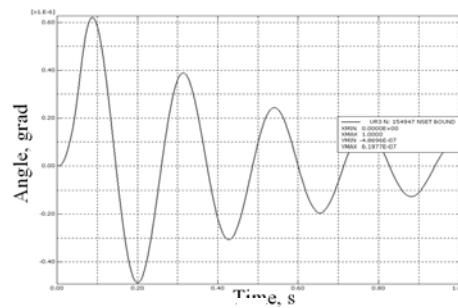


Figure 17. Damping at u_{ϕ_z} .

3. Special computers used for analysis

As it was noted in the Introduction, creation of this paper would not have been feasible without the efficient cluster of JSC Atomenergoproekt, because multiple solutions of the large size problem with account of nonlinear factors were necessary.

This cluster consists of four nodes, servers DELL PowerEdge 2950 of the following configuration: 2 four-nuclear processors Intel Xeon 3 GHz with main memory of 64 Gbyte; Infiniband bus is used for organization of operative inter-processor interaction between cluster nodes;

For storage of big volume of data generated in the course of calculations, cluster is connected to storage disc system EMC CX4-120 via bus FiberChannel.

Cluster is controlled via Gigabit Ethernet network. Operative system RedHat Enterprise Linux 4.6 operate in cluster nodes.

4. Mathematic model of the soil-structure system

In order to carry out dynamic analyses the spatial mathematic model of the building was developed with the account of its complicated spatial structure, with due respect for inertia, and in some cases stiffness properties of equipment. Soil with regard to AC was accounted through springs and dampers, which simulate the equivalent stiffness and damping. The mathematic model of the reactor building features the following:

- total number of finite elements (FE) is 78898;
- total number of nodes is 72114;
- total number of degrees of freedom is 429840.

The following FE types were used in the simulation:

- shell/plate element *S4R* for simulation of walls, floors and shells;
- beam element *B31* for simulation of the reactor,
- concentrated mass element *MASS* for account of equipment components not developed in the model in details,
- spring element *SPRING2* for account of soil stiffness,
- damper element *DASHPOT2* for account of energy dispersion into soil.
- noteworthy that in this study the integral springs and dampers were connected to surface of the foundation slab accounted as rigid body, in its geometric centre.

Sections along row B and along axis 3 of finite-element scheme of the building are shown in Figure 18 and 19, and points of aircraft shocks are shown in Figure 20, 21 and 22.

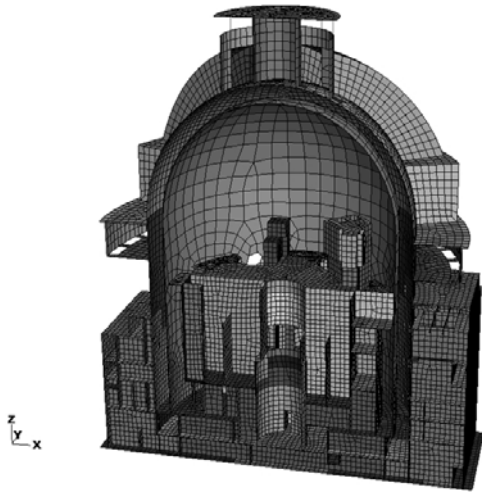


Figure 18. Fragment of finite-element scheme, section is cut along row B.

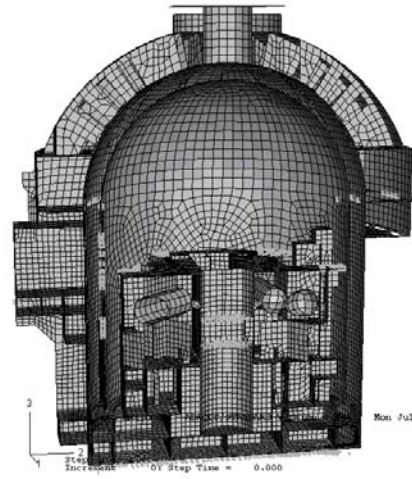


Figure 19. Fragment of finite-element scheme, section is cut along axis 3.

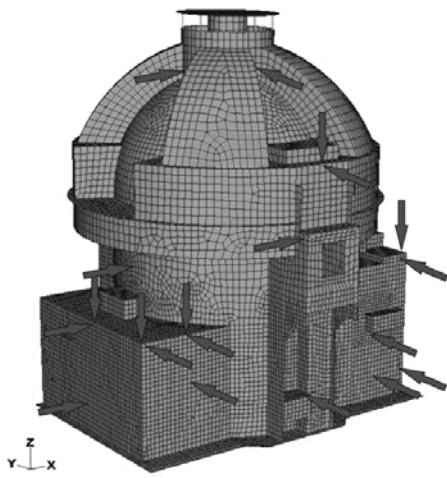


Figure 20. Points of aircraft shocks.

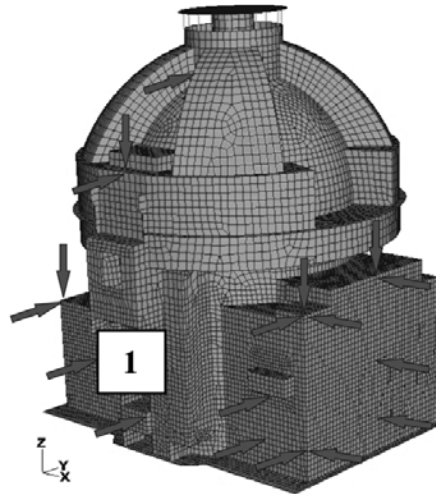


Figure 21. Points of aircraft shocks.

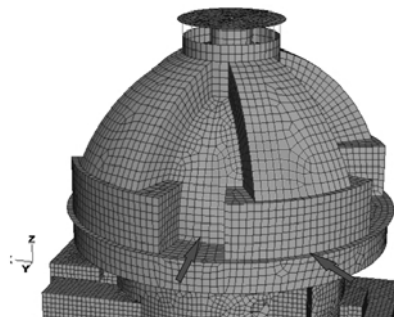


Figure 22. Points of aircraft shocks.

For reinforced concrete structures there was used concrete *B50* for outer structures (shells and building annex), *B25* (extra-heavy concrete) for hermetic area and *B25* for the other structures as well as *Class A500* rebars. Characteristics of concrete are indicated in Table 4.

Table 4. Characteristics of reinforced concrete structures of the reactor compartment.

Class of concrete	Modulus of elasticity (tonne/m ²)	Calculated concrete resistance R_t (t/m ²) for axial tension	Reinforced concrete density (tonne/m ³)
<i>B50</i>	$3.9 \cdot 10^6$	$8.3 \cdot 10^2$	2.5
<i>B25</i> (extra-heavy concrete)	$3.25 \cdot 10^6$	-	3.6
<i>B25</i>	$3.06 \cdot 10^6$	-	2.5

Rebars feature the following: pitch is 200 mm, diameter is 1.26 cm, elastic modulus is $2.1 \cdot 10^7$ t/m², Poisson's ratio is 0.3, yield point is 50000 t/m², ultimate limit is 62000 t/m² when strain reaches 0.005. It shall be pointed out that in ABAQUS the longitudinal reinforcement is accounted as layers with the reduced characteristics of material.

5. Main results

The model of nonlinear strain of concrete 'Brittle Cracking Model' was applied only for outer surfaces of the structure, internals of the model were in elastic realm of strain. The Brittle Cracking Model was applied in ABAQUS/Explicit (calculation according to the explicit integration scheme) is recommended in case cracking occurs mostly during tension, and compression behaviour is of elastic nature. Functionality of the concrete model discussed here was checked in the test task. Plate of 25 25 m size, 0.5 m thick restrained along the perimeter was studied. Impulse caused by crash of Phantom was applied to the centre of plate, and timing characteristic of displacement was defined in the centre of this plate. Comparison between results of ABAQUS calculation and calculation don according to UDAR code [3] is shown in Figure 23. One can see good concurrence of results for nonlinear behaviour of material in Figure 23.

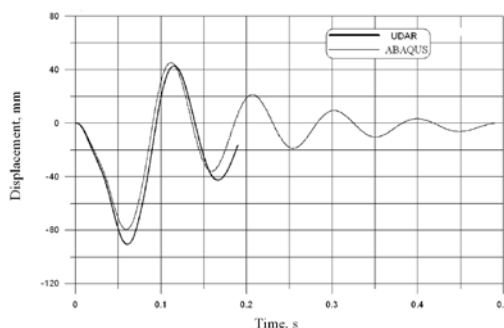


Figure 23. Comparative analysis of displacements obtained in both ABAQUS and UDAR within the test task.

Response spectra in equipment locations

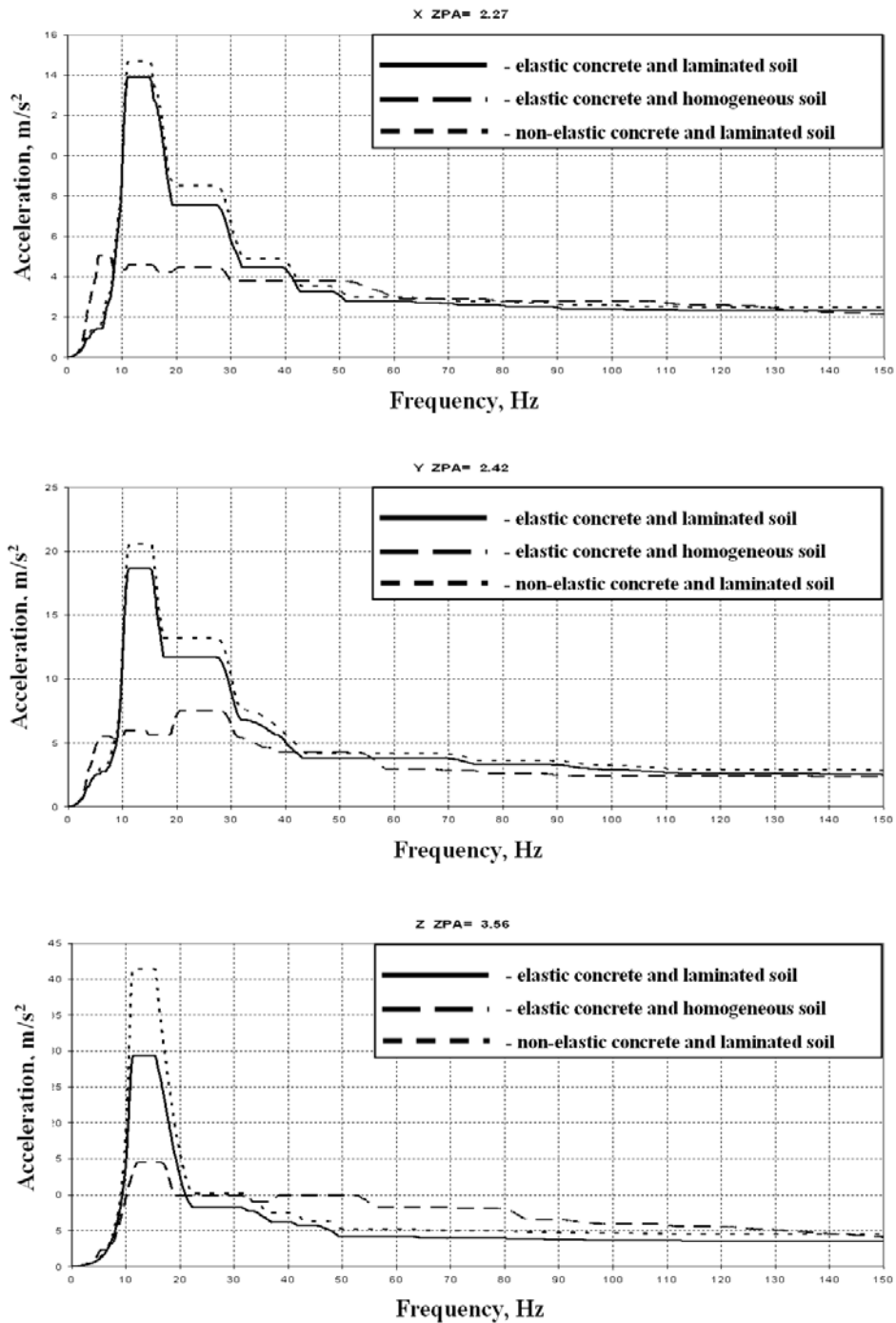


Figure 24. Non-hermetic area. Expanded enveloping response spectra caused by AC. Foundation slab. Elevations -7.200 m and -4.200 m in axes 1p-5p.

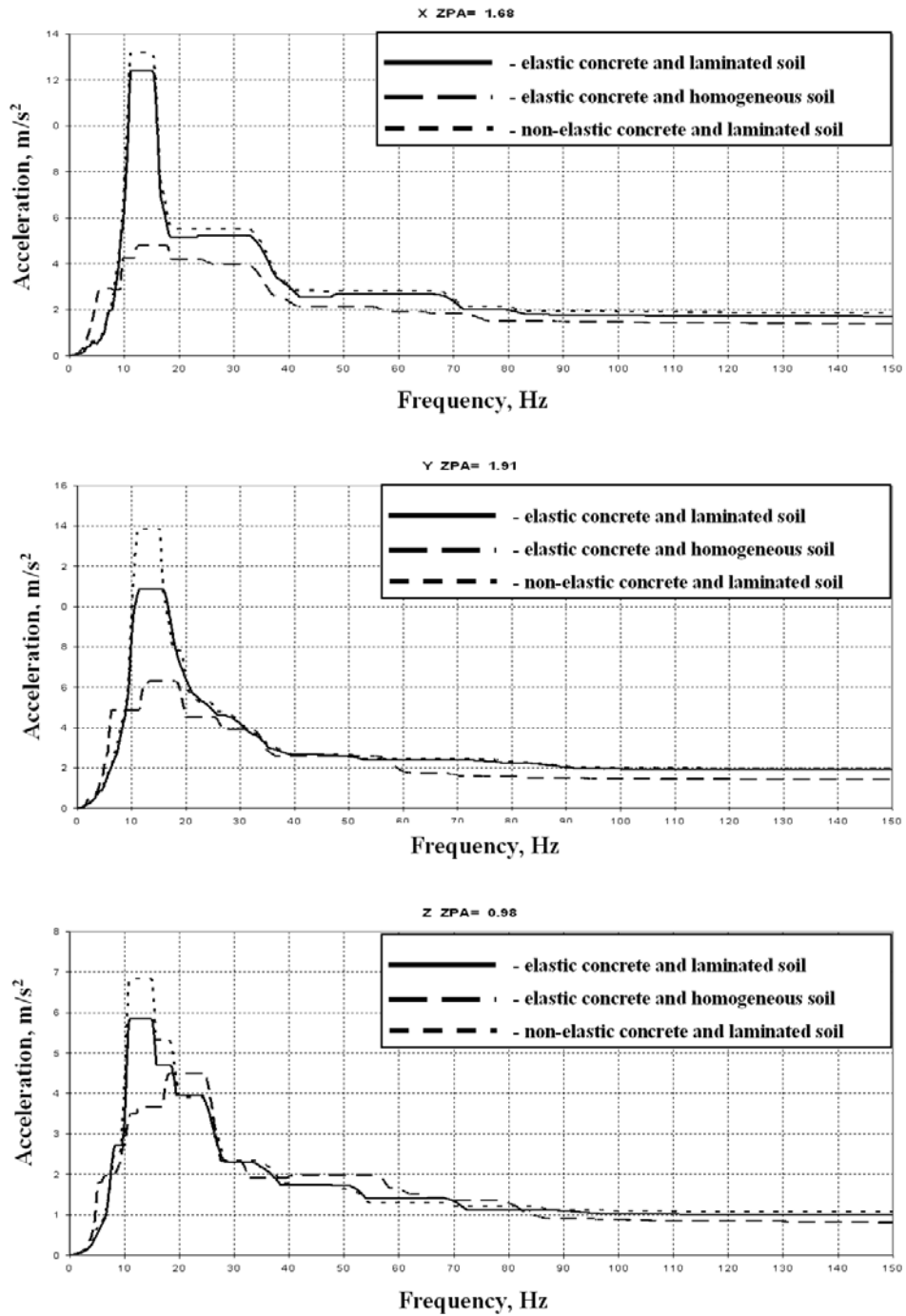


Figure 25. ALA. Expanded enveloping response spectra caused by AC at elevation +17.100 m. Reactor bottom support ring.

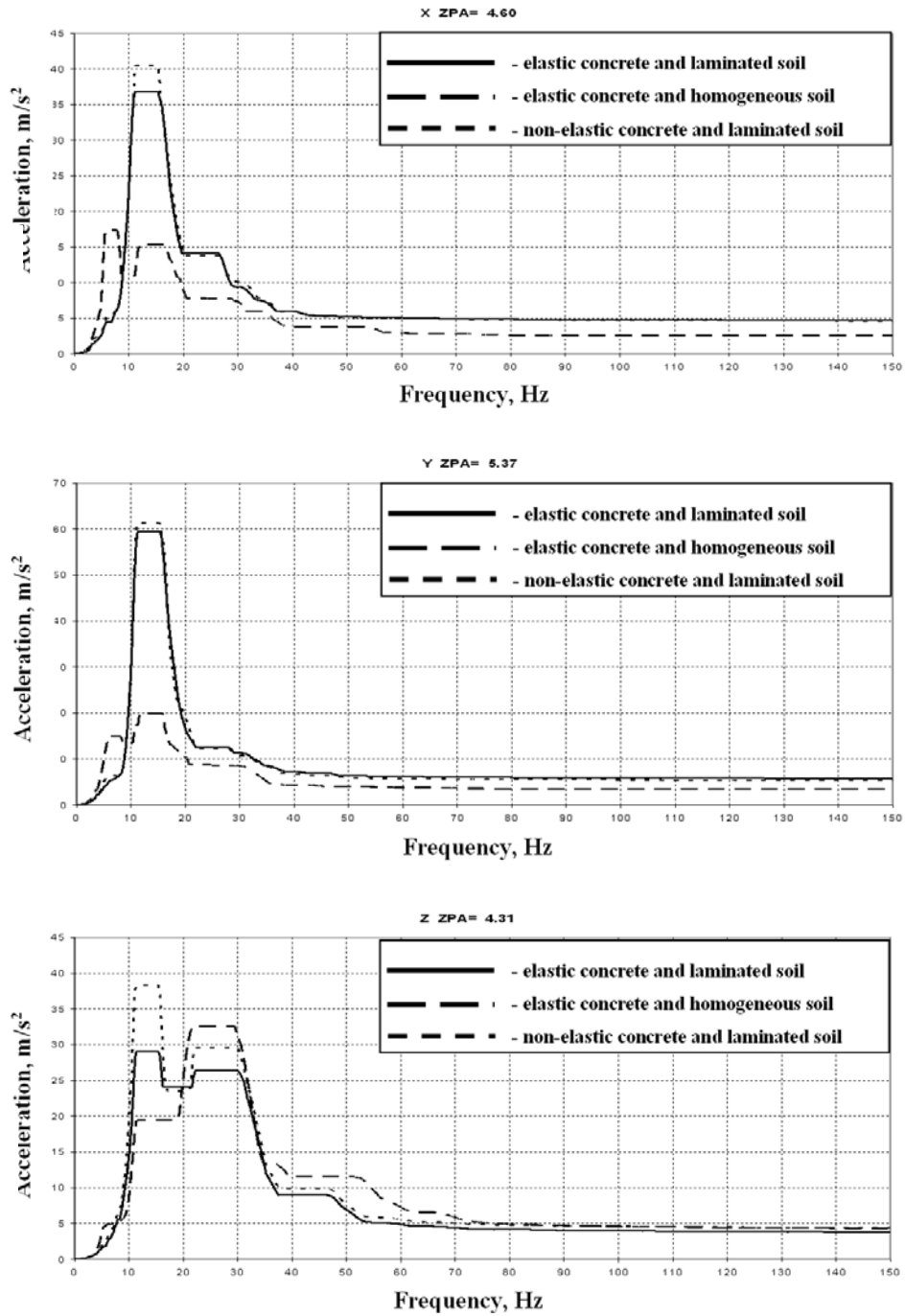


Figure 26. ALA. Expanded enveloping response spectra caused by AC at elevation +31.700 m. Except for ASCPF accumulators and pressurizer room.

As a result of calculation according to the explicit integration scheme, the response spectra were determined in equipment locations. In Figure 24,25 and 26 comparisons of response spectra are given for 2% damping for three analyses:

- elastic concrete and laminated soil;
- elastic concrete and homogeneous soil;
- non-elastic concrete and laminated soil in case of shock 1 shown in Figure 21.

Comparative review of results proves that accounting of non-elastic behaviour of concrete leads mainly to essential drop of spectral accelerations. In some cases some growth of spectra still occurs. It happens because of varying frequency composition of the structure in case of inelastic deformation of concrete, which causes resonances. The most conservative results are obtained for the homogeneous soil and elastic behaviour of concrete.

6. Conclusions

1. Here we propose the method of analysis of response spectra in civil structures of nuclear plant caused by aircraft crash with account of laminated soil basis and nonlinear strain of reinforced concrete in the shock area.
2. In the framework of this method the review of comparisons between the equivalent stiffness and damping of soil and the results obtained in ASCE, and review of comparisons between nonlinear strain of reinforced concrete obtained in ABAQUS and UDAR codes confirm veracity of the proposed approach.
3. Review of comparison between the resulting response spectra obtained with inelastic behaviour of concrete and laminated soil base and the response spectra obtained for elastic model of concrete and homogeneous soil basis proves that spectral accelerations decreases up to three times. Influence of soil lamination is also essential, since being compared with homogeneous soil (ASCE), spectral accelerations decreases down to 40%.
4. According to opinion of authors the presented approach based on static stiffness and logarithmic damping decrement for account of soil basis lamination can also be used in seismic analyses.

7. References

1. "ASCE4-98. ASCE Standard. Seismic Analysis of Safety Related Nuclear Structures and Commentary," Approved 1998.
2. V.A. Korotkov, D.V. Kapustin, "Method of Determination of Response Spectra in Civil Structures of Nuclear Plants in Case of Seismic Events," Collection of FSUE Atomenergoproekt's Proceedings, Edition No.6, 2006.
3. V.I. Golyakov, "Verification Calculation with the Use of UDAR code," Atomenergoproekt, 2007, Arch.No. 2380.